An Experimental Study on Static and Cyclic Undrained Behaviour of Gangetic Sand

S. Sharika[1] · S. D. Anitha Kumari[1]

Abstract Earthquake disasters in seismically active zones revealed the phenomenon of liquefaction which plays a key role in monitoring its severity. Liquefaction affects the stability of the soil by reducing the effective stress which makes soil flows like a liquid. Cohesionless soils under undrained conditions are highly vulnerable to liquefaction, whose effect will be added if it is nearer to the river basin. The present paper investigates the performance of Gangetic sand obtained from the Indo-Gangetic River basin by examining its static and dynamic behavior using triaxial tests. Static as well as cyclic trials were extended for similar three confining pressures and two different densities. The static behavior of the Gangetic Sand was examined on the basis of stress–strain, effective stress path, and pore pressure generation. In addition to the above, the evolution of cyclic stress ratio and dynamic properties including degradation of shear modulus and damping coefficient were analysed while assessing the cyclic behavior. The effect of loading conditions, density, pressures, state of the soil, and stress history were also explored in the current paper.

✉ S. Sharika
sharika2091@gmail.com

S. D. Anitha Kumari
anithakumari.ce.et@msruas.ac.in

[1] Department of Civil Engineering, M.S. Ramaiah University of Applied Sciences, Bangalore, India

Introduction

Liquefaction studies became more prominent after the devastating earthquakes occurred in Niigata and Alaska in the year 1964 [1]. The phenomenon of liquefaction refers to the sudden decrease in the shear strength of soil due to a rapid increase in pore water pressure under undrained conditions. This sudden change usually occurs during dynamic loading like earthquakes, which in turn decreases intergranular stresses or effective stress and thereby the shear strength. Once the shear strength is lost, the soil will behave like a liquid and thereby failure of structures resting on it. It is noted that liquefaction in the field can occur under both static and cyclic loading conditions and hence it is mandatory to analyze both loading conditions. As the soil is heterogeneous, it takes a long time to figure out the exact behaviour under loading. For the past several decades, research is going on in this field to predict the potential of liquefaction with different techniques including empirical & semi-empirical [2, 3], analytical [4–6], Experimental [7–15], and numerical techniques [16] as a countermeasure. From the identified methods, the present report focuses on experimental techniques for analyzing soil behavior. Experimental studies replicate the actual field conditions fairly well and also are useful for the identification of soil parameters easily. The laboratory results can be used as a reference in other fields also to simulate the results analytically or numerically. Experimental studies on liquefaction have validated with diverse techniques including triaxial tests, simple shear tests, shake table tests, resonant column tests, etc. where the present study looks forward to the simulations of static and cyclic triaxial tests for analyzing the liquefaction potential of Gangetic sand. Though some of the recent studies have explored the behaviour of Gangetic River sand, a combined

study on the static as well as cyclic behaviour was rarely examined. Thus, the present paper has given a unified framework for identifying the static as well as the dynamic behaviour of Gangetic sand in the context of liquefaction. Along with that, the current research also investigated the cyclic behaviour by studying evolution of dynamic soil properties which are crucial for identifying the generalized soil behaviour.

Experimental Program

Properties of Sand

The studies were conducted on alluvial soils of the Gangetic plains. Around 75 kg of soil samples were collected from the river banks of Solani situated in Roorkee which is developed around the banks of the Ganges with the help of Central Building Research Institute (CBRI), Roorkee. The area comes under seismic zone III and is found to be vulnerable to liquefaction. Recent studies on this area also analyzed its susceptibility to earthquake damages [16, 18] and emphasizes the importance of mitigation methods. From the basic tests conducted, the specific gravity of the sand is found to be 2.65, with maximum and minimum densities of 1.62 g/cc and 1.36 g/cc respectively. The corresponding void ratios are noticed as 0.62 and 0.94. The particle size distribution curve of Gangetic sand along with the boundary limits for liquefaction [19] is shown in Fig. 1. It is clear that the Gangetic soil lies within the boundary limits and is highly susceptible to liquefaction. It is also inferred that the coefficient of uniformity (C_u) is 2 and the coefficient of curvature (C_c) is 1.13. Since the value of $C_u < 4$ and C_c is between 1 and 3, as per IS classification the soil sample is poorly graded and uniform.

Fig. 1 Grain size distribution of Gangetic Sand and boundary limits of liquefaction (Source: Iwasaki [19])

Specimen Preparation

Static as well as dynamic trials were conducted on soil samples by maintaining an aspect ratio of 1:2. Aspect ratio refers to the ratio of diameter to length which is a key factor for the triaxial tests. Dry pluviation, water pluviation, vibratory techniques, moist tamping, and other sample reconstitution methods have been identified to play a crucial role in determining liquefaction resistance as per the literature survey [20, 21]. Among them, the moist tamping method was identified to show better liquefaction resistance which provides a higher remoulded strength compared with other techniques [22]. It will produce a metastable bulked honeycomb structure that led to exaggerated contractive behavior during saturation, consolidation, and shearing [23–25]. Analyzing the importance, for the current study, moist tamping method was adopted for sample preparation.

Test Procedure

The samples were prepared using a split spoon sampler with a vacuum-sucking arrangement. Once the sample preparation is over, the triaxial cell is filled with water and ready for testing. Stages adopted for trials include saturation, consolidation, and shearing. A small confining pressure was applied to make the sample stable (nearly 30 kPa) and Carbon-di-oxide (CO_2) gas at a pressure of less than 5 kPa is passed for nearly 45 min through the backpressure valve. By doing so, CO_2 having higher solubility will dissolve the air present in the soil voids so that time required for complete saturation can be reduced effectively. It is then followed by water flushing, where the back pressure pipe is connected to the sample and a volume of nearly thrice the volume of the sample (nearly 500 ml) has been collected, to increase the rate of saturation. Then, cell pressure (CP) and back pressure (BP) have given in increments once in 2 h with an effective stress difference of 20 kPa. Skempton's pore pressure parameter (B) was monitored continuously to ensure the degree of saturation and is assumed to be satisfied once the value reached 0.95. Saturation is followed by consolidation where required effective stress is applied to the sample and is assumed to terminate once the volume change is less than 0.1 ml for nearly 30 min. The shearing stage for static tests is conducted using a static triaxial machine under a strain rate of 0.6 mm/min and cyclic trials were conducted with an automated cyclic triaxial device under a frequency of 1 Hz and with an amplitude of 0.4 mm.
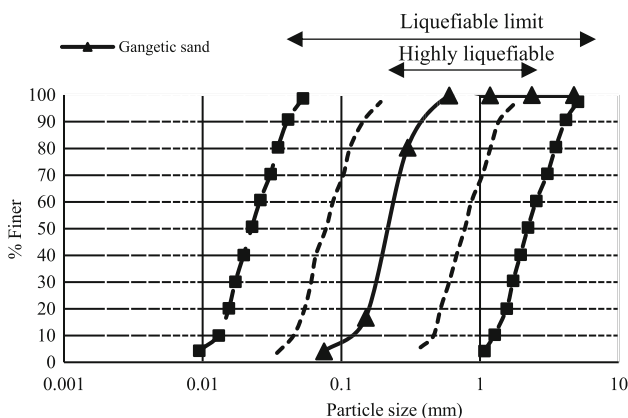
Static Undrained Behavior of Gangetic Sand

The static undrained behavior of Gangetic sand is studied in the context of stress–strain, stress path variation, and the generation of pore pressure. A strain rate of 0.6 mm/min is adopted for the trials. Detailed interpretation of the results is discussed in the next section.

Results and Discussion

Consolidated undrained (CU) tests as per [26] were conducted on 2 relative densities 20% and 80%, under 3 different confining pressures 50 kPa, 100 kPa and 200 kPa. Results were analyzed in critical state framework and thus the tests were extended to an axial strain up to 20%. The densities were chosen to keep the samples in loose and dense conditions [27]. The range of confining pressures is selected to identify the soil behavior in a minimal to moderate confined state and also keep in mind liquefaction is a low-pressure phenomenon [17]. Figure 2 shows the stress–strain behavior of loose samples followed by their stress paths and pore pressure effects. It can be observed that as the confining pressure becomes high, the shear strength of soil also increased. From the lowest confining stress, i.e. 50 kPa to the highest stress 200 kPa, the maximum deviatoric stress value has increased nearly double (300 to 600 kPa). In addition, instead of a markable difference in stress–strain behavior for the early stages of loading, the ultimate state attained by the samples under large deformation is identical independent of confining pressure which is stated as the critical state or steady-state [28, 29]. At critical state, samples will undergo continued deformation with no increase in shear stress irrespective of the state of the sample and loading conditions. Also, samples attain a minimum strength at a strain of less than 5% and are referred to as the quasi-steady-state [7], which is a temporary condition that may change with the initial con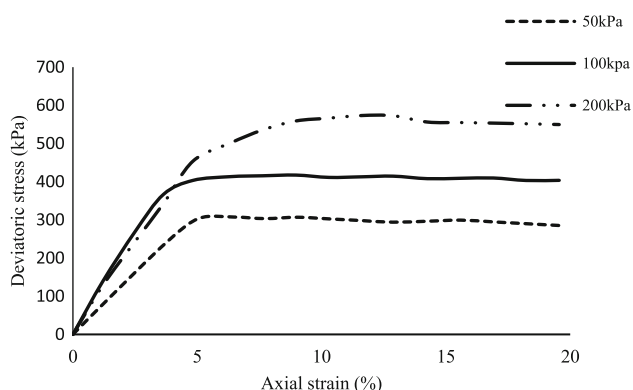solidation pressures. It is been reported that this state is strongly affected by the initial fabric and the structure of soil mass. Again, for 50 and 100 kPa pressures, the sample failure was observed at nearly 5% of axial strain while for the 200 kPa, the failure happened at 10%. This could be attributed to the effect of increased confining stress, which gave the soil additional stability.

Reduction in effective stress plays a key role in liquefaction predictions and is examined in the effective stress space (p'-q) which is shown in Fig. 3. The capacity of soil to resist applied load at any stage and the stress changes in the soil state is best represented by the p'-q space. The intensity of liquefaction under three pressures is calculated based on Liquefaction potential (Lp) [23], by incorporating steady-state concepts and is computed in terms of effective minor principal stress at the initial and final stage of shearing. It was observed that for 50 and 100 kPa, the Lp value was found to be 50 and 99 respectively while for the 200 kPa it is calculated as 23. From the literature survey, it is stated that Lp more than 24 is susceptible to liquefaction [17]. However, as the deviatoric stress value is not reached zero, a complete liquefaction vulnerability cannot be stated for the soil. In terms of instability, Gangetic sand's behavior can be characterized as a condition of temporary instability [8]. It is defined as a state in which the undrained stress difference reaches a maximum value before declining to a minimum value. This decrease is due to a rise in pore pressure as a result of prolonged shearing. Thus, it is concluded that Gangetic sand is prone to limited liquefaction under small confining stresses and is stable if the confining stress is high. Regardless of the confining pressures, all samples in the loose state exhibit contractive behavior, resulting in a reduction in the sample's effective stress.

Pore pressure ratio (PPR) generation during shearing has a very high impact on analyzing liquefaction characteristics which is shown in Fig. 4. Results show that the pore pressure ratio reaches 1 for applied confining stress of 50 and 100 kPa pressures, which also gives an idea of the vulnerability of soil under low pressures. However, an
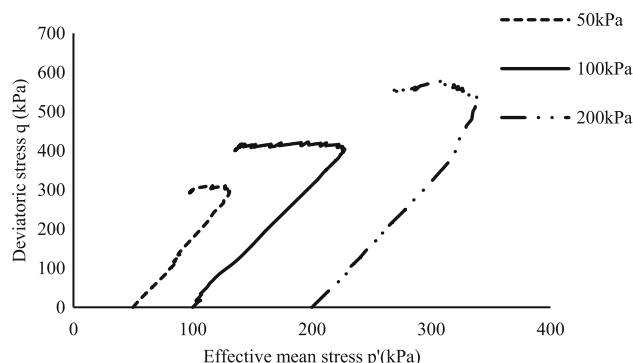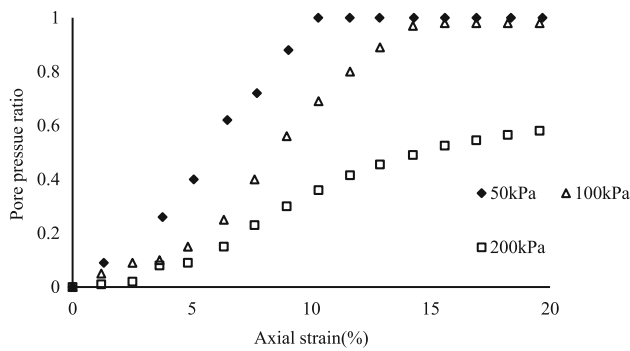
Fig. 2 Stress–Strain response of loose samples

Fig. 3 Effective stress path for loose samples

Fig. 4 Variation of Pore pressure ratio with axial strain for loose samples

Fig. 6 Effective stress paths of dense samples

increase in confining stress offers more stability to the soil which is identified by the minimal pore pressure ratio under 200 kPa.

The soil behaviour at the densest condition with ($Dr = 80\%$) is shown in Fig. 5. It is noted that, unlike the loose samples, the samples in dense state exhibited a strain-softening behaviour with a sharp peak in deviatoric stress value followed by a steady decrease under continued deformation. Also, the peak values for the confining pressures 50 and 100 kPa are found nearly equal which might be due to the influence of density under shearing. However, the effect of confining stress can also be validated from the graph as the peak value increases with an increase in confining stress. Again, similar to the loose state, the failure strain was observed to be in a range of 5–12%, and the soil ultimately reaches critical state [28] on further shearing.

Unlike the loose samples, dense samples show a dilative behaviour which is best identified from the p'-q space given in Fig. 6. An increase in effective stress from the beginning of shearing is observed for the samples irrespective of the confining pressures applied. It is thus concluded that if the soil is dense, the liquefaction susceptibility is negligible. As the dilation strongly
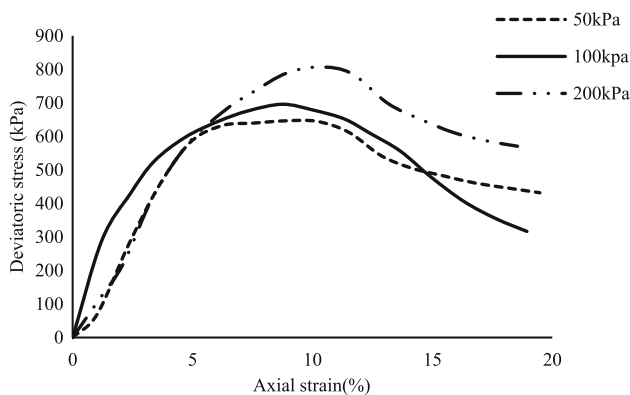
depends on the stress history of the soil, from the literature data [30], it can be stated that the soil under this particular density is in an over-consolidated state.

Pore pressure ratio (PPR) generation during shearing for the dense state is shown in Fig. 7. Though there is an increase in PPR during the initial stage of shearing, as the loading progresses it decreased to zero and then started increasing in the negative direction. This phenomenon also indicates the dilative tendency of the soil in dense state. Again, all the samples reached minimal positive pressures under a failure strain of less than 10%.

Cyclic Liquefaction Characteristics of Gangetic Sand

Mechanism of Cyclic Liquefaction

Under undrained cyclic loading conditions, sand particle rearrangement occurs which results in the transfer of normal stresses from soil skeleton to the pore water. Though the total stress remains constant, this results in a reduction in effective stress due to an increase in pore water pressure. Dynamic loading also induces plastic strains which are counterbalanced by the elastic expansion of the sand

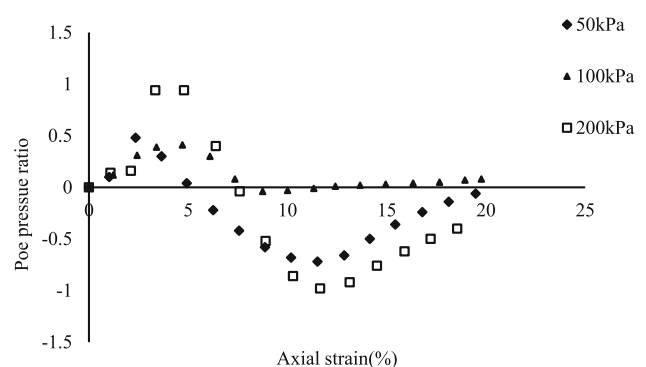Fig. 5 Stress–strain response for dense samples

Fig. 7 Variation of Pore pressure ratio with axial strain for dense samples

skeleton under reduced effective stress. In the worst scenario, the applied cyclic loading will break apart the sand-to-sand contacts resulting in zero contact stress and thereby zero shear strength [17]. Thus, in the limiting case, all the stresses are carried by the pore water pressure with u equal to σ and the state of liquefaction is reached.

Methods and Methodology

Cyclic triaxial tests can be either done in stress-controlled or strain-controlled mode [31]. Though literature is surplus with both types [9] of loading, [17, 32] it was mentioned that the strain-controlled tests are more accurate in the realistic prediction of in-situ pore pressures and cause only less water content redistribution compared with stress-controlled tests and also the fabric effect on pore pressure is negligible if the strain-controlled tests are done [33]. An Automated cyclic triaxial system, shown in Fig. 8 is adopted for the current study. The cell and back pressures were applied through the air–water interface mechanism with the help of a compressor. A pore pressure transducer was connected at the bottom of the specimen to measure the generating pore pressure. Volume change during saturation and consolidation was recorded through a sensitive volume change device with an accuracy of 0.1 ml. All pressure applications, measurement of pore pressure, volumetric change, and load values were controlled and recorded in the automatic data acquisition system. A submersible load cell of 10 kN capacity and accuracy of 1 N was connected to the top of the specimen. The LVDT of stroke length $\pm$ 10 mm and an accuracy of 0.001 mm were connected to the top of the specimen. A sinusoidal waveform of a given frequency (f) and amplitude (A) is applied as input loading. The output in the form of variations in load and pore pressure was recorded in the data acquisition system at the intervals of 10 ms. For the present study 1 Hz


Fig. 8 Cyclic triaxial apparatus used for the present study (Courtesy: Sarathy Geotech Lab Pvt.Ltd)

frequency and 0.4 mm amplitude is used, which is adopted for replicating earthquake loading conditions.

Results and Discussion

The dynamic behavior of Gangetic sand presented in the context of stress–strain, effective stress path, and pore pressure ratio is presented in this section. Samples in the loosest state with *(Dr = 20%)* and dense state with *(Dr = 80%)* [27] were tested for three different confining pressures 50 kPa, 100 kPa, and 200 kPa. The range of confining pressures and densities was taken similarly as that of the static trials. The behavior under lower confining stresses 50 kPa and 100 kPa. Figure 9a & b nearly show a similar behavior unless in the peak deviatoric stress values but when the confining pressure increased to 200 kPa the sample was found to be more stable under dynamic loading as shown in Fig. 9c. For the 50 kPa, it was observed that the behavior is highly unstable, and also a well-defined curve is not obtained. It can be seen that even for the first cycle of loading, the deviatoric stress value is very less, (nearly 5 kPa) which shows the severity under loose and lower confining stresses where the sample is vulnerable to liquefaction. It is also observed that the load-carrying capacity has decreased from 5 to 1 kPa within 5 cycles of dynamic loading. This negligible value is attributed to the lesser cyclic strength, and nearly 50% reduction in the shear modulus even for initial loading cycles. The effective stress plot, in Fig. 10a shows that at the end of approximately 6 cycles of loading, the mean stress value nearly reaches zero. This reduction of shear stress is attributed to liquefaction, where the sample is subjected to loss of shear strength under dynamic loading. The results for 100 kPa in Fig. 10b also show a similar trend except in the deviatoric stress value. The deviatoric stress value (q) increased to 120 kPa on the first cycles of loading which reduced to a minimal value within 8–10 cycles. For the 1st cycle of loading, the maximum value was found to be 55 kPa and degraded to a minimum value within 10 cycles of loading. The mean effective stress also becomes negligible after initial cycles which is identified as complete liquefaction. However, for the 200 kPa, shown in Fig. 10c the deviatoric stress value (q) increased to 120 kPa on the first cycles of loading which reduced to a minimal value within 8–10 cycles. The mean effective stress on the sample has not reached zero which indicates the sample hasn't experienced liquefaction but rather undergone a strength degradation of 87%. However as the reduction is nearly close to liquefaction, it is expected that further shearing makes samples liquefy. Again, as it is observed for the same density, it might be due to the effect of higher confining stress which gives soil added stability. Again, as per the literature survey, [1, 34, 35] pore pressure ratio greater than
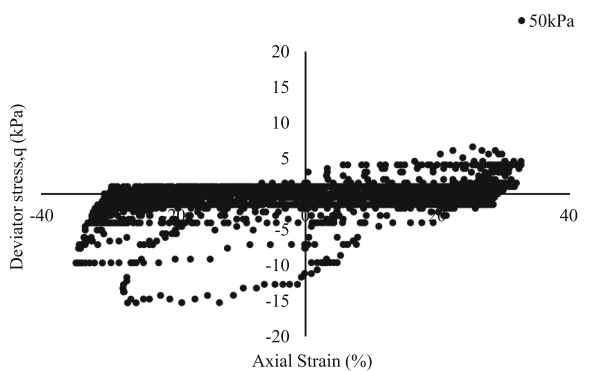
(a) Stress-Strain behaviour of loose samples for 50kPa
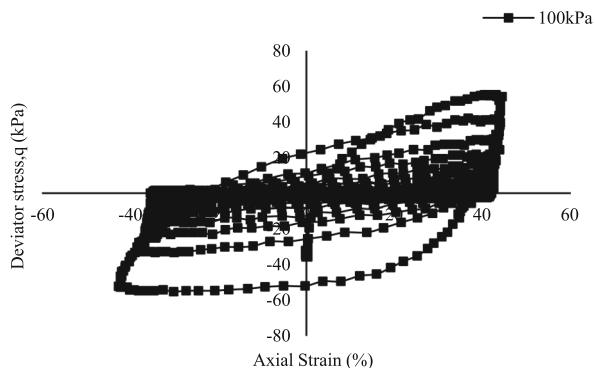
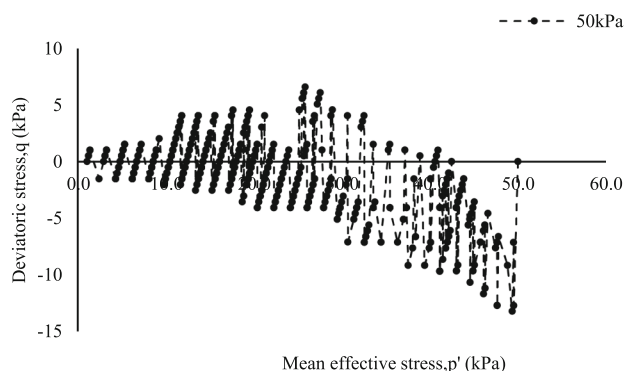**(b) Stress-Strain behaviour of loose samples for 100kPa**
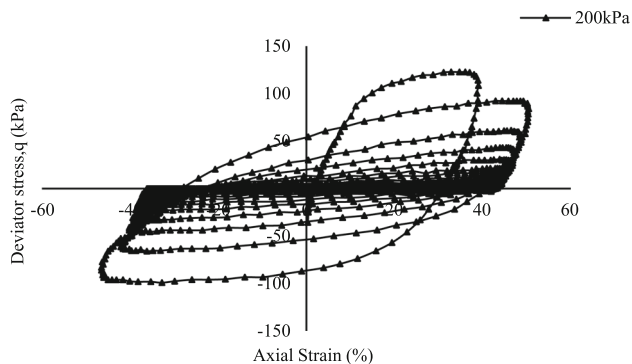
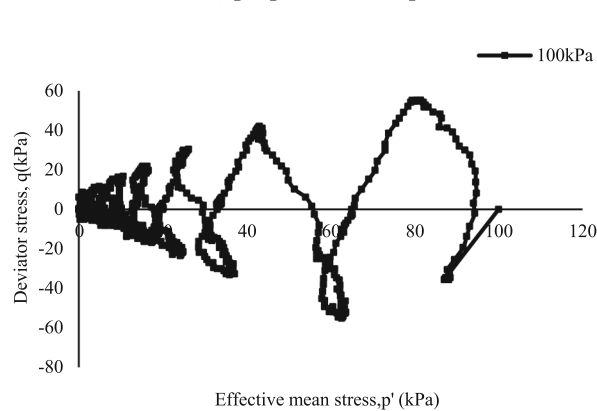**(c) Stress-Strain behaviour of loose samples for 200kPa**

Fig. 9 a Stress–Strain behaviour of loose samples for 50 kPa. **b** Stress–Strain behaviour of loose samples for 100 kPa. **c** Stress–Strain behaviour of loose samples for 200 kPa

(a) p'-q of loose samples for 50kPa

(b) p'-q of loose samples for 100kPa

(c) p'-q of loose samples for 200kPa

Fig. 10　a p'-q of loose samples for 50 kPa. **b** p'-q of loose samples for 100 kPa. **c** p'-q of loose samples for 200 kPa

0.9 is critical when analyzed from the context of lique-faction, and the same is observed at less than 10 cycles of loading. It is detected that the pore pressure ratio reached more than 0.95 for 50 and 100 kPa pressures within 8–15 cycles (Fig. 11a & b) while it was observed that for 200 kPa the maximum value has reached only 0.87(Fig. 11c).
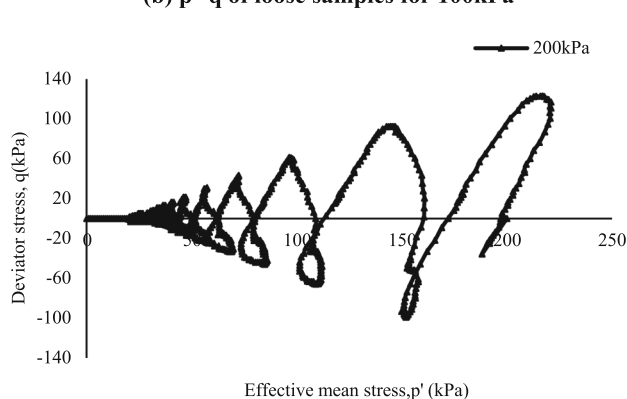
Figure 12a & b shows the stress–strain behavior of Gangetic sand for relative density *(Dr = 80%)* under con-fining pressures of 50 and 100 kPa. Samples with lower

confining stress exhibit complete liquefaction within 10–15 cycles of loading. The same is verified by observing the p'-q plot also where the deviatoric stress value reaches zero after initial cycles of loading shown in Fig. 13a & b. The pore pressure ratio exceeded 0.95 within 10 loading cycles which are plotted in Fig. 14a & b. However, for the 200 kPa confining pressure, it is noted that the deviatoric stress has increased to a higher value (Fig. 12c). The effective stress of the sample, shown in Fig. 13c hasn't reached zero even after 50 loading cycles which also shows
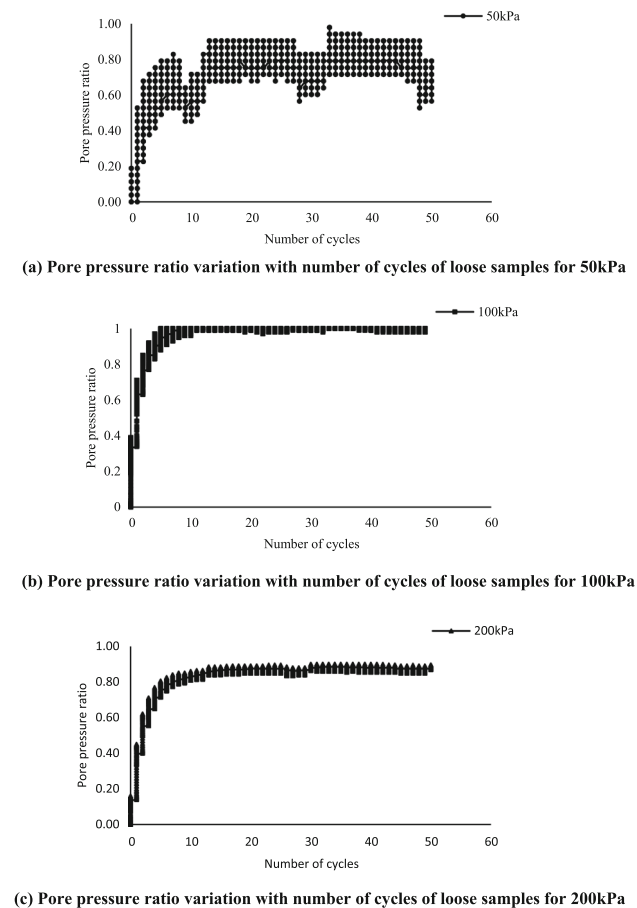
(a) Pore pressure ratio variation with number of cycles of loose samples for 50kPa

(b) Pore pressure ratio variation with number of cycles of loose samples for 100kPa

(c) Pore pressure ratio variation with number of cycles of loose samples for 200kPa

Fig. 11 a Pore pressure ratio variation with number of cycles of loose samples for 50 kPa. **b** Pore pressure ratio variation with number of cycles of loose samples for 100 kPa. **c** Pore pressure ratio variation with number of cycles of loose samples for 200 kPa

the influence of confining stress under dynamic loading. Similarly, the pore pressure ratio has only reached a maximum value of 0.75, shown in Fig. 14c also validated the increase in liquefaction resistance with confining stress. In addition, the effect of density also can be substantiated by analyzing the dense and loose behavior for the lowest confining pressure. The deviatoric stress value has changed from 5 to 30 kPa in the initial cycles for the 50 kPa, however irrespective of density there hasn't been any notable difference observed for the other two confining stresses.

Cyclic Strength Reduction of Gangetic Sand

The dynamic behaviour of Gangetic sand is also examined in terms of reduction in cyclic strength by examining the evolution of the cyclic stress ratio. Cyclic strength curves are those which show the relationship between density, cyclic stress amplitude, and number of cycles to liquefaction failure which is expressed graphically by interpreting
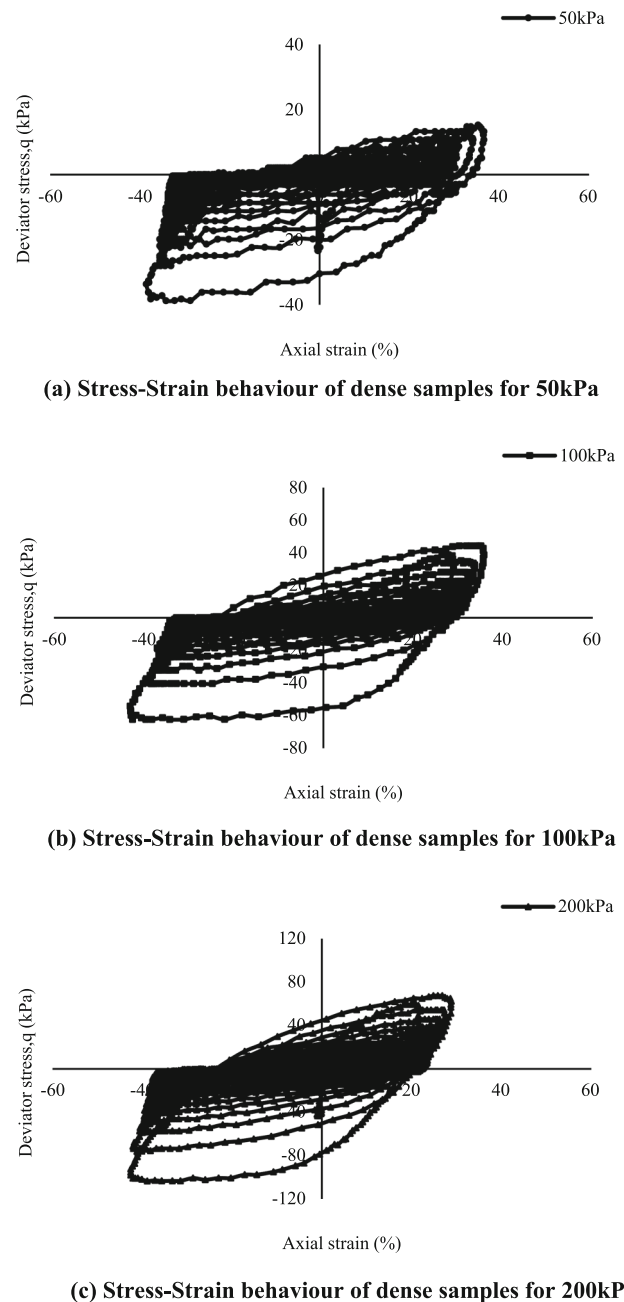

(a) Stress-Strain behaviour of dense samples for 50kPa

(b) Stress-Strain behaviour of dense samples for 100kPa

(c) Stress-Strain behaviour of dense samples for 200kPa

Fig. 12 a Stress–Strain behaviour of dense samples for 50 kPa. **b** Stress–Strain behaviour of dense samples for 100 kPa. **c** Stress–Strain behaviour of dense samples for 200 kPa

laboratory results. These curves are normalized with the initial effective pressure gives the cyclic stress ratio [36]. The cyclic strength curve is obtained by plotting the cyclic stress ratio evolved for various cycles with number of cycles. The onset condition of liquefaction is defined as the amount of cyclic stress ratio required to produce 5% double-amplitude axial strain in 20 cycles of uniform load application, which is referred to as cyclic shear strength, based on the cyclic strength curve [7]. A comparison of the
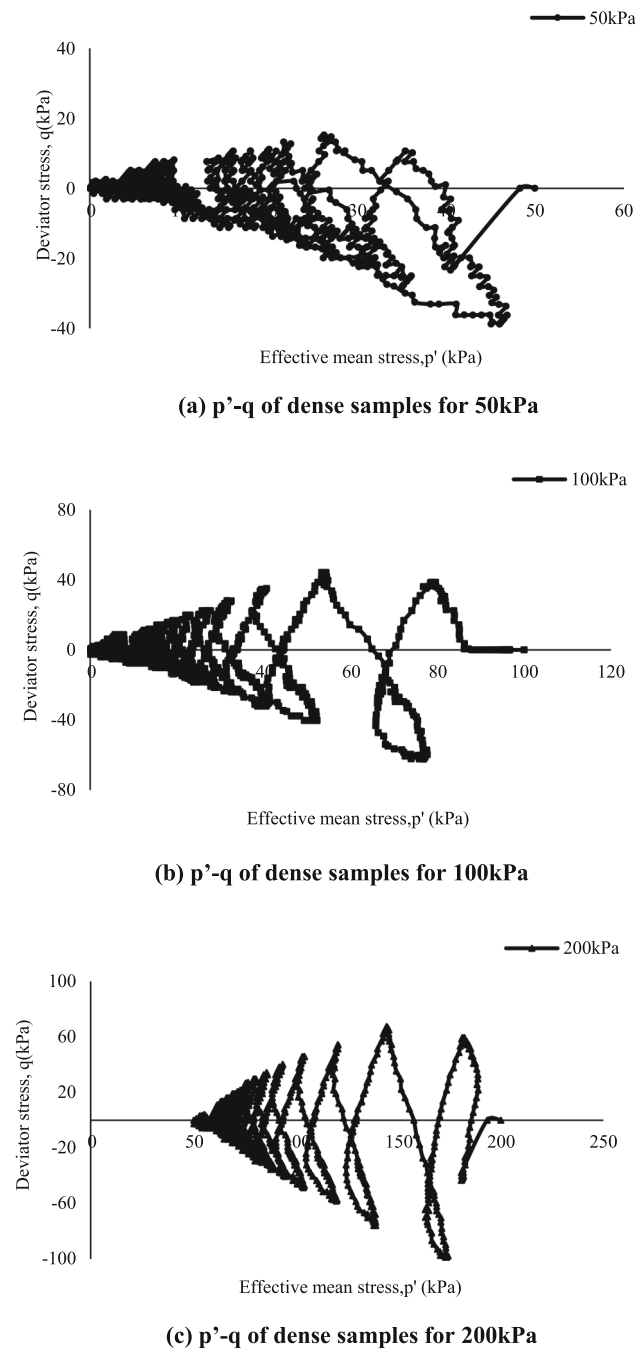
(a) p'-q of dense samples for 50kPa

(b) p'-q of dense samples for 100kPa

(c) p'-q of dense samples for 200kPa

Fig. 13 a p'-q of dense samples for 50 kPa. b p'-q of dense samples for 100 kPa. c p'-q of dense samples for 200 kPa

(a) Pore pressure ratio variation of dense samples with number of cycles for 50kPa

(b) Pore pressure ratio variation of dense samples with number of cycles for 100kPa

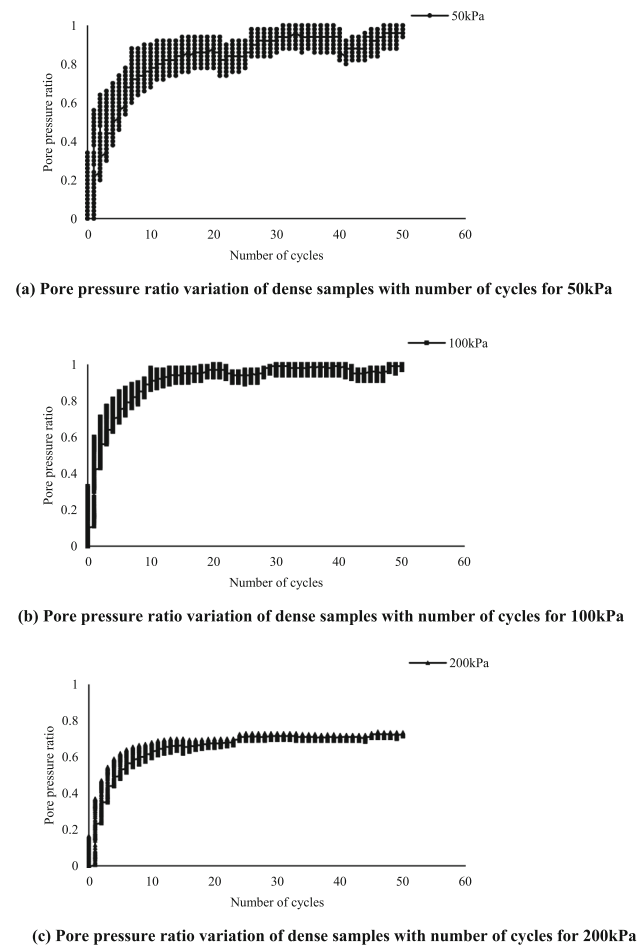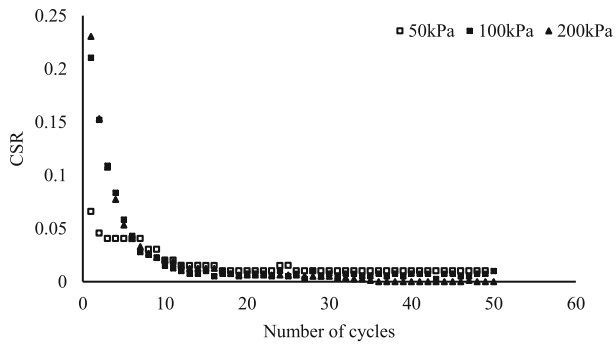(c) Pore pressure ratio variation of dense samples with number of cycles for 200kPa

Fig. 14 a Pore pressure ratio variation of dense samples with number of cycles for 50 kPa. b Pore pressure ratio variation of dense samples with number of cycles for 100 kPa. c Pore pressure ratio variation of dense samples with number of cycles for 200 kPa
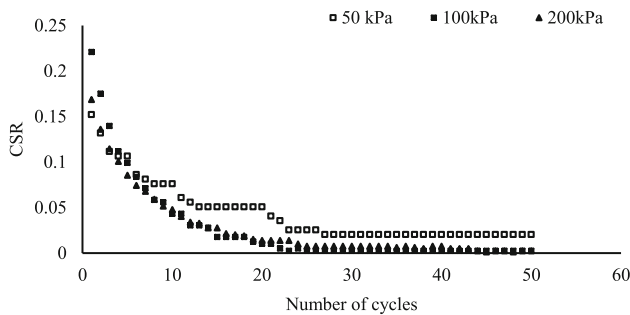
maintained constant and had a strong resemblance with the stress–strain, effective stress, and pore pressure ratios. This reduction in strength after initial cycles of loading is owing to the collapsible metastable interparticle structure of the soil particles under dynamic loading conditions [25].

Dynamic Properties of Gangetic Sand

The response of the soil subjected to dynamic loading is governed by the dynamic soil properties including modulus reduction and damping [2, 37]. A soil subjected to dynamic loading exhibits hysteresis response, whose locus of tip points is called the backbone or skeleton curve. Its slope at the origin represents the largest value of shear modulus (G_{max}). The slope of the loop with variation in strains is characterized by the secant shear modulus (G_{sec}). At higher strains, the modulus ratio (G_{sec}/G_{max}) drops and its variation in the shear strain is characterized by the modulus reduction curve (Kramer, [36]) This modulus reduction can

evolution of the cyclic stress ratio (CSR) for the loose and dense state is shown in Fig. 15a & b. While analyzing the evolution of CSR for the loose and dense state it is observed that for the loose state, the CSR for all samples varied from 1 to 0.01 irrespective of the confining pressures. However, a CSR variation of 1–0.04 is observed in the dense state for the 50 kPa pressure which is again reduced to 0.01 for the other two pressures. In general conclusion, after 20 cycles of loading, the CSR is

(a) CSR Evolution of loose samples

(b) CSR Evolution of dense samples

Fig. 15 a CSR Evolution of loose samples. b CSR Evolution of dense samples

(a) Shear of modulus degradation loose samples

(b) Shear modulus degradation of dense samples

Fig. 16 a Shear of modulus degradation loose samples. b Shear modulus degradation of dense samples

also be expressed in terms of degradation index(δ_N), where the variation of shear modulus with the number of cycles is analyzed [38].
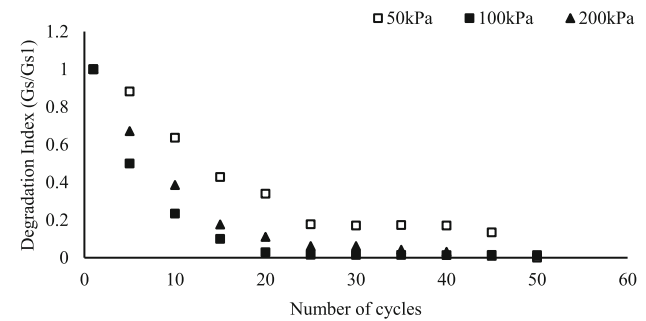
$$\delta_N = G_S/G_{S1} \tag{1}$$

where G_S is the secant shear modulus at "N" number of cycles and G_{S1} is the secant shear modulus during the first cycle. Figure 16a & b shows the modulus degradation curve for Gangetic sand in loose and dense state. This degradation shows a strong resemblance with the CSR evolution and becomes negligible once it attained the state of liquefaction. Though the 200 kPa samples exhibited cyclic degradation, the shear modulus reached a zero value after 50 cycles of loading.

Damping describes the energy dissipated by soils under dynamic loading which affects the soil-structure interaction and ground response significantly during cyclic loading. It represents the ability to dissipate dynamic load or dampen the system. The major factors which influence the damping include the frequency and amplitude of loading, relative density, mean effective stress, number of cycles and void ratio, method of sample preparation, confining pressure, etc. The damping coefficient is calculated based on the following equation given [31] and the area of hysteresis loop is calculated using MATLAB software. The variation

of damping coefficient with the number of cycles is plotted in Fig. 17a & b shown below

$$D = \frac{A_L}{4\pi A_T} \times 100 \tag{2}$$

where, D = material damping coefficient in % A_L = Area of hysteresis loop (dissipated energy). A_T = Area of shaded right triangle (maximum strain energy).

It was noted that the looser samples exhibited a complete reduction in the damping coefficient for 100 and 200 kPa samples while for all the confining pressures, denser samples reached a minimum value of 10%. This behavior may be due to the effect of relative density where the void ratio was minimal for the denser state which exhibits a lower rate of energy dissipation with number of cycles.

Comparison of Results with Reported Literature

Liquefaction susceptibility of both clayey as well as sandy soils has been analyzed by various researchers in the past. Though static liquefaction studies are rare, dynamic analyses were reported pretty much. Out of them, three relevant researches on sand were compared with current work to check for precision and accuracy.
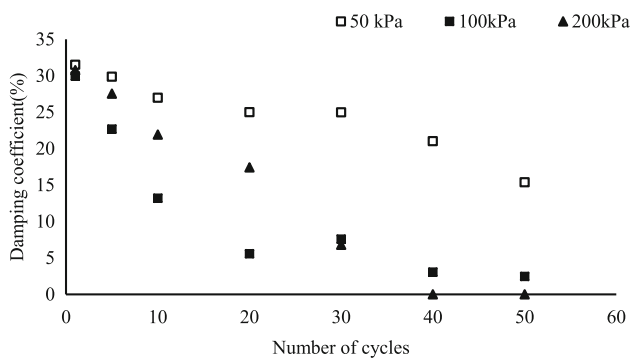
(a) Variation of damping coefficient for loose samples
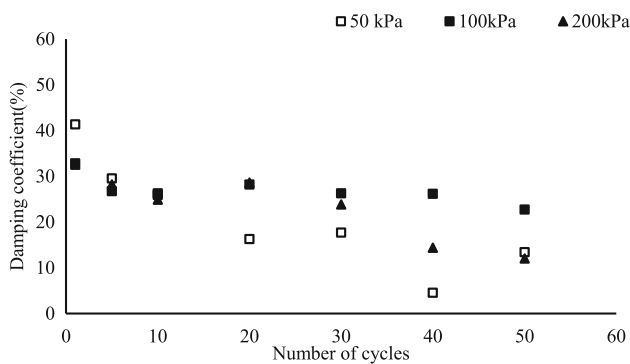
(b) Variation of damping coefficient for dense samples

Fig. 17 a Variation of damping coefficient for loose samples. **b** Variation of damping coefficient for dense samples

To identify the general behaviour of liquefiable soils, the static and dynamic behaviour of Kutch soils [17] were analyzed. Though the static behaviour was not comparable, dynamic results, especially the CSR variation of Gangetic sand is identical with the Kutch region. For Kutch soils, majority of the samples got liquefied within 30 cycles of loading. As the author already mentioned, the presence of fines affects the liquefaction susceptibility, the comparatively higher cycles for the strength reduction might be attributed to the silty nature of Kutch sand.

Experimental studies on dense samples (RD = 50%) of Solani river sand [16] which is from the Gangetic plain region under dry and saturated conditions are compared with present tests. The behavior exhibited for monotonic loading conditions closely matches the current trials. The strength was found to be marginally higher for the Solani sand, however, the variation of p-q as well as the pore pressure generation was nearly uniform for both soils. While analyzing the dynamic soil behavior, Solani sand showed a higher liquefaction resistance for the initial loading cycles under the same confining pressure. However, all the samples failed within 6 cycles of loading which is close to the number of cycles taken by the current sand.

Results of a recent study conducted on 3 different grains of sand [39] collected from the Indo-Gangetic region are assessed with the current trials. Among them, samples from Allahabad city show comparable results with the present research. The strength characteristics as well as effective stress path results were almost alike for both sands. The influence of density as well as the confining pressure observations were also found to be similar.

Conclusion

The present paper examines the static and cyclic undrained behaviour of Gangetic sand in the context of liquefaction. Samples were prepared for two relative densities 20% and 80% and tested under three different confining pressures 50 kPa, 100 kPa, and 200 kPa. The stress–strain, effective stress path, and pore pressure behavior of Gangetic sand were investigated under static conditions. Results have revealed that the state of soil and the confining stress plays a key role in liquefaction susceptibility. Loose samples under lower confining stress (50 and 100 kPa) were found to be vulnerable while dense samples due to their dilation were observed to be safe against liquefaction. For the dynamic trials also, a nearly uniform behavior was observed for the loose and dense samples under lower confining stresses, while a greater strength reduction is observed for the higher pressure. In addition, the evolution of CSR as well as its dynamic properties were evaluated. The cyclic strength curve as well as shear modulus reduction has given a clear idea regarding the vulnerability of Gangetic sand to liquefaction. The paper thus concludes that for static loading conditions, loose Gangetic sand is vulnerable to liquefaction under lower confining stresses. Under dynamic loading, irrespective of density, samples with lower confining stress exhibit liquefaction within 10–15 cycles, while 200 kPa samples show only strength reduction even after 50 loading cycles. It has been deduced that those samples might liquefy if the number of loading cycles has increased. Also, expectant results from these trials can be taken for the field correlations to identify the effective stress influence if the sample depth is known.

Declarations

Conflict of interest All authors declare that we have no conflict of interest to disclose.

References

1. Ishihara K (1993) Liquefaction and flow failure during earthquakes. Geotechnique 43:351–415. https://doi.org/10.1680/geot.1993.43.3.351

2. Seed HB, Wong RT, Idriss IM, Tokimatsu K (1986) Moduli and damping factors for dynamic analysis of cohesionless soils. J Geotech Eng 112:1016–1032. https://doi.org/10.1061/(ASCE)0733-9410(1986)112:11(1016)

3. Tokimatsu K, Yoshimi Y (1981) Field correlation of soil liquefaction with SPT and grain size. In: Proceeding 1st Internationaal Conference on recent advances in geotechnical earthquake engineering and soil dynamics, pp 203–208

4. Zhang B, Muraleetharan KK, Liu C (2016) Liquefaction of unsaturated sands. Int J Geomech. https://doi.org/10.1061/(asce)gm.1943-5622.0000605

5. Andrianopoulos KI, Papadimitriou AG, Bouckovalas GD (2010) Bounding surface plasticity model for the seismic liquefaction analysis of geostructures. Soil Dyn Earthq 30:895–911. https://doi.org/10.1016/j.soildyn.2010.04.001

6. Boukpeti N, Mroz Z, Drescher A (2002) A model for static liquefaction in triaxial compression and extension. Can Geotech J 39:1243–1253. https://doi.org/10.1139/t02-066

7. Verdugo R, Ishihara K (1996) The steady state of sandy soils. Soils Found 36:81–91. https://doi.org/10.3208/sandf.36.2_81

8. Yamamuro JA, Lade PV (1997) Static liquefaction of very loose sands. Can Geotech J 34:905–917. https://doi.org/10.1139/t97-057

9. Dinesh SV, Kumar GM, Balreddy GM, Swamy BC (2011) Liquefaction potential of Sabarmati river sand. ISET J Earthq Technol 48:61–71

10. Castro G (1965) Liquefaction of sands. Dissertation, Harvard University, Cambridge, Massachusetts

11. Kokusho T (2016) Major advances in liquefaction research by laboratory tests compared with in situ behavior. Soil Dyn Earthq Eng 91:3–22. https://doi.org/10.1016/j.soildyn.2016.07.024

12. Kumar SS, Dey A, Krishna AM (2020) Liquefaction potential assessment of Brahmaputra sand based on regular and irregular excitations using stress-controlled cyclic triaxial test. KSCE J Civ Eng 24:1070–1082. https://doi.org/10.1007/s12205-020-0216-x

13. Della N, Arab A, Belkhatir M (2011) Static liquefaction of sandy soil: an experimental investigation into the effects of saturation and initial state. Acta Mech 18:175–186. https://doi.org/10.1007/S00707-010-0410-X

14. Hussain M, Sachan A (2019) Static liquefaction and effective stress path response of Kutch soils. Soils Found 59:2036–2055. https://doi.org/10.1016/j.sandf.2019.11.004

15. Sitharam T, Ravishankar BV, Patil SM (2012) Liquefaction and porepressure generation in sand: cyclic strain controlled triaxial tests. Int J Geotech Earthq Eng 3:57–85. https://doi.org/10.4018/IJGEE.2012010104

16. Kanth A, Maheshwari BK (2021) Monotonic and cyclic loading behaviour of Solani sand: experiments and finite element simulations. Int J Geotech Eng. https://doi.org/10.1080/19386362.2021.1966225

17. Hussain M (2019) Static and cyclic liquefaction characteristics of Kutch soils. Dissertation, IIT Gandhinagar

18. Kirar B, Maheshwari BK, Jakka RS (2012) Dynamic properties of solani sand reinforced with coir fibers

19. Iwasaki T (1986) Soil liquefaction studies in Japan: state-of-the-art. Soil Dyn Earthq Eng. https://doi.org/10.1016/0267-7261(86)90024-2

20. Ladd RS (1974) Specimen preparation and liquefaction of sands. J Geotech Geoenviron Eng 100:1180–1184. https://doi.org/10.1061/AJGEB6.0000117

21. Tatsuoka F, Ochr K, Fum OM (1986) Cyclic undrained triaxial and torsional shear strength of sands for different sample preparation methods. Soils Found 26:23–42. https://doi.org/10.3208/sandf1972.26.3_23

22. Mulilis JP, Chan CK, Seed HB (1975) The effects of method of sample preparation on the cyclic stress–strain behaviour sands. Tech Rep Univ Calif Berkeley 103:91–108. https://doi.org/10.1016/0148-9062%2877%2990060-21

23. Casagrande A (1975) Liquefaction and cyclic deformation of sands-a critical review. Harvard Soil Mechanics Series

24. Vaid YP, Thomas J (1995) Liquefaction and post liquefaction behaviour of sand. J Geotech Eng 121:163–173. https://doi.org/10.1061/(ASCE)0733-9410(1995)121:2(163)

25. Hussain M, Sachan A (2019) Dynamic characteristics of natural Kutch sandy soils. Soil Dyn Earthq Eng. https://doi.org/10.1016/j.soildyn.2019.105717

26. ASTM D4767-95 Standard test method for consolidated undrained triaxial compression test for cohesive soils 1. ASTM Int. West Conshohocken, PA

27. Budhu M (2011) Soil mechanics and foundations, 3rd edn. USA, Wiley

28. Schofield A, Wroth P (1968) Critical state soil mechanics. McGraw-Hill, London

29. Jefferies M, Been K (2016) Soil liquefaction: a critical state approach, 2nd edn. CRC Press, Boca Raton

30. Djafar HA, Arab A, Belkhatir M, Hamoudi AS, Khelafi H (2011) Undrained behavior of silty sand: effect of the overconsolidation ratio. Arab J Geosci 6:297–307. https://doi.org/10.1007/s12517-011-0365-9

31. ASTM D3999/3999M-11 standard test methods for the determination of the modulus and damping properties of soils using the cyclic triaxial apparatus 1', ASTM Int. West Conshohocken, PA

32. Ishihara K, Tatsuoka F, Yasuda S (1975) Undrained deformation and liquefaction of sand under cyclic stresses. Soils Found. https://doi.org/10.3208/SANDF1972.15.29

33. Seed B, Silver ML (1971) Volume changes in sands during cyclic loading. J Soil Mech Found Div 97:1171–1182

34. Du S, Chian SC (2017) Excess pore pressure generation in sand under non-uniform cyclic strain triaxial testing. Soil Dyn Earthq Eng 109:119–131. https://doi.org/10.1016/j.soildyn.2018.03.016

35. Hazirbaba K, Omarow M (2019) Strain-based assessment of liquefaction and seismic settlement of saturated sand. Cogent Eng 6:1–16. https://doi.org/10.1080/23311916.2019.1573788

36. Kramer SL (1996) Geotechnical earthquake engineering, Prentice-Hall Series

37. Maheshwari BK, Kale SS, Kaynia AM (2015) Dynamic properties of Solani sand under cyclic loads. 14SEE, https://www.researchgate.net/publication/265427284

38. Idriss IM, Dobry R, Sing RD (1978) Nonlinear behavior of soft clays during cyclic loading. J Geotech Geoenviron Eng 104:1427–1447

39. Naik SP, Patra NR, Malik JN (2022) Cyclic behavior of late quaternary alluvial soil along Indo-Gangetic Plain: Northern India. Geo-Engineering. https://doi.org/10.1186/s40703-021-00167-y